Journal of Magnetic Resonance 305 (2019) 51–57

Contents lists available at ScienceDirect

Journal of Magnetic Resonance

journal homepage: www.elsevier.com/locate/jmr

Sensitivity analysis of magic angle spinning dynamic nuclear polarization below 6 K

Patrick T. Judge [a,b], Erika L. Sesti [a], Edward P. Saliba [a], Nicholas Alaniva [a], Thomas Halbritter [c], Snorri Th. Sigurdsson [c], Alexander B. Barnes [a,*]

[a] Department of Chemistry, Washington University in St. Louis, One Brookings Drive, St. Louis, MO 63130, USA
[b] Department of Biochemistry, Biophysics & Structural Biology, Washington University in St. Louis, St. Louis, MO 63110, USA
[c] Department of Chemistry, University of Iceland, Science Institute, Dunhaga 3, 107 Reykjavik, Iceland

ARTICLE INFO

Article history:
Received 30 January 2019
Revised 28 May 2019
Accepted 30 May 2019
Available online 4 June 2019

Keywords:
Dynamic nuclear polarization
Cryogenic magic angle spinning
Helium driven MAS

ABSTRACT

Dynamic nuclear polarization (DNP) improves signal-to-noise in nuclear magnetic resonance (NMR) spectroscopy. Signal-to-noise in NMR can be further improved with cryogenic sample cooling. Whereas MAS DNP is commonly performed between 25 and 110 K, sample temperatures below 6 K lead to further improvements in sensitivity. Here, we demonstrate that solid effect MAS DNP experiments at 6 K, using trityl, yield 3.2× more sensitivity compared to 90 K. Trityl with solid effect DNP at 6 K yields substantially more signal to noise than biradicals and cross effect DNP. We also characterize cross effect DNP with AMUPol and TEMTriPol-1 biradicals for DNP magic angle spinning at temperatures below 6 K and 7 Tesla. DNP enhancements determined from microwave on/off intensities are 253 from AMUPol and 49 from TEMTriPol-1. The higher thermal Boltzmann polarization at 6 K compared to 298 K, combined with these enhancements, should result in 10,000× signal gain for AMUPol and 2000× gain for TEMTriPol-1. However, we show that AMUPol reduces signal in the absence of microwaves by 90% compared to 41% by TEMTriPol-1 at 7 Tesla as the result of depolarization and other detrimental paramagnetic effects. AMUPol still yields the highest signal-to-noise improvement per unit time between the cross effect radicals due to faster polarization buildup (T_{1DNP} = 4.3 s and 36 s for AMUPol and TEMTriPol-1, respectively). Overall, AMUPol results in 2.5× better sensitivity compared to TEMTriPol-1 in MAS DNP experiments performed below 6 K at 7 T. Trityl provides 6.0× more sensitivity than TEMTriPol-1 and 1.9× more than AMUPol at 6 K, thus yielding the greatest signal-to-noise per unit time among all three radicals. A DNP enhancement profile of TEMTriPol-1 recorded with a frequency-tunable custom-built gyrotron oscillator operating at 198 GHz is also included. It is determined that at 7 T below 6 K a microwave power level of 0.6 W incident on the sample is sufficient to saturate the cross effect mechanism using TEMTriPol-1, yet increasing the power level up to 5 W results in higher improvements in DNP sensitivity with AMUPol. These results indicate MAS DNP below 6 K will play a prominent role in ultra-sensitive NMR spectroscopy in the future.

1. Introduction

Magic angle spinning (MAS) nuclear magnetic resonance (NMR) spectroscopy is a high-resolution technique capable of providing not only site-specific structural information in biomolecules, pharmaceuticals, and materials, but also information on the dynamics of the system relating to its function [1–5]. However, NMR is typically sensitivity limited due to a weak nuclear spin Zeeman interaction compared to thermal energy [6–8]. Dynamic nuclear polarization (DNP) can overcome this limitation by transferring large electron spin polarization to nuclear spins of interest [9–18]. At high magnetic fields suitable for site-specific NMR resolution, this transfer is achieved with the use of high frequency microwave sources [19–25].

The most common mechanism employed in continuous wave DNP with MAS is the cross effect [26,27]. The cross effect is active when the electron paramagnetic resonance (EPR) lineshape of the polarizing agent is dominated by inhomogeneous interactions, and the combined lineshape of all of the radicals that make up the polarizing agent is wider than the Larmor frequency of the nucleus to be polarized [28–30]. However, in the absence of

* Corresponding author.
E-mail address: barnesab@wustl.edu (A.B. Barnes).

https://doi.org/10.1016/j.jmr.2019.05.011
1090-7807/© 2019 Published by Elsevier Inc.

microwave irradiation, level crossings at the cross effect matching conditions are still present and can depolarize nuclei, leading to signal-to-noise ratios considerably lower than the Boltzmann case seen in the absence of radical [28–32]. Therefore the large gains in sensitivity from cross effect DNP must often be analyzed in the context of detrimental effects arising from the DNP polarizing agents. The AMUPol binitroxide radical is one of the most common polarizing agents for cross effect DNP, yet has been shown to depolarize as much as 60% under MAS at 100 K [28,33,34].

Radicals have been developed that avoid depolarization while still allowing for the cross effect, thereby improving overall sensitivity [29,34,35]. One such radical is TEMTriPol-1, which contains a trityl radical tethered to a mononitroxide radical [29,36]. The higher symmetry of the trityl g-tensor results in less inhomogeneous broadening, and attenuates detrimental level crossing which can result in depolarization [29]. The degree of depolarization of TEMTriPol-1 has previously been characterized at 100, 110, and 125 K [29].

MAS DNP is typically performed at temperatures near 100 K, but there is a large desire to access MAS below 25 K [19,37,39–43]. Among other benefits, DNP-NMR signal-to-noise ratios are improved at lower temperatures due to higher Boltzmann polarization of the electron spins and longer electron spin relaxation resulting in more efficient DNP transfers [41,42].

Here, we investigate the behavior of DNP radicals including trityl, TEMTriPol-1 and AMUPol at temperatures below 6 K and at a magnetic field of 7 T. We characterize the sensitivity with respect to signal-to-noise per unit time. For cross effect DNP, we also measure the nuclear longitudinal relaxation times (T_1), polarization build-up times (T_{1DNP}), maximum enhancements, and depolarization effects. The DNP enhancement profile of TEMTriPol-1 is also recorded with MAS at 90 K, as is the microwave power dependence of biradicals with MAS at 6 K and 90 K.

2. Experimental methods

2.1. Sample preparation

Samples were prepared with 4 M [U-^{13}C,^{15}N] urea (Cambridge Isotope Laboratories, Tewksbury, MA) and 5 mM radical AMUPol (Cortecnet, Voisins-le-Bretonneux, France), 5 mM TEMTriPol-1, or 40 mM Trityl Finland radical (Oxford Instruments, Abingdon, UK) in a d_8-glycerol/D_2O/H_2O mixture at a 60/30/10 vol ratio. An identical radical-free sample was also prepared. Once mixed, approximately 36 μL of each sample was packed into 3.2 mm zirconia rotors, and spun in a custom-built MAS DNP spectrometer [22,38,44].

2.2. MAS-DNP-NMR spectroscopy

Electron polarization from biradicals was transferred to nearby protons via the cross effect using continuous wave (CW) microwave irradiation, and the bulk protons were polarized via spin diffusion [16]. The microwave irradiation frequency was 197.670 GHz for TEMTriPol-1, 197.674 GHz for AMUPol, and 197.719 GHz for the Trityl Finland radical. Polarization transfer with cross polarization (CP) was achieved with $\omega_{1H}/2\pi = 50$ kHz, $\omega_{13C}/2\pi = 52$ kHz, and a Hartmann-Hahn contact time of 1 ms. The ^{1}H Larmor frequency was 300.179 MHz, and the ^{13}C Larmor frequency was 75.494 MHz at a $B_0 = 7.05$ T. All data were recorded with a custom-built, four-channel, 3.2 mm, transmission line MAS-NMR probe using a Redstone spectrometer (Tecmag Inc., Houston, TX) [44]. Rotor-synchronized, echo-detected, CPMAS sequences were used to record all data. A nutation of $\omega_{1H}/2\pi = 90$ kHz was used for π/2 pulses and TPPM decoupling on ^{1}H [48]. A nutation of $\omega_{13C}/2\pi = 100$ kHz was used for the ^{13}C refocusing pulse to generate Hahn echoes. Magnetization was saturated with a train of pulses on both ^{1}H and ^{13}C prior to the DNP polarization time (τ_{pol}). The τ_{pol} was 3 s to measure the enhancement profile of TEMTriPol-1. The τ_{pol} for all other experiments was 1.26 * T_{1DNP}. A saturation recovery sequence was used to measure the longitudinal nuclear relaxation times with no microwave irradiation (T_1), and also polarization build-up times with microwave irradiation (T_{1DNP}). Spinning frequencies were between 5600 and 5800 Hz with ±40 Hz stability, and exact details of spinning are described in respective figure captions. Microwave irradiation generated from custom-built 198 GHz gyrotrons was coupled to the sample using corrugated waveguides, tapers, and mirrors [22,44]. The gyrotron output was 40 W, with approximately 7 W incident on the sample [22,23,44].

Enhancements were determined by taking the ratio of signal intensity recorded with microwave irradiation and without microwave irradiation, taking into account scaling required by the number of scans used for each experiment. DMFit was used to fit the peaks and determine the areas and intensities. [45] For power dependence measurements, the microwave power was varied with attenuators placed within the waveguide (Tydex LLC, St. Petersburg, Russia), and microwave power was measured using a custom-built water calorimeter.

To achieve sample temperatures below 6 K, liquid helium was used as a variable temperature (VT) fluid directed at the center of the spinning zirconia rotor [37]. Ultra-high purity helium gas at 80 K was used for bearing and drive. The sample temperature was monitored at the interface of the VT outlet and NMR stator with a calibrated Cernox temperature sensor (Lake Shore Cryotronics, Inc., Westerville, OH). This temperature represents the sample temperature as previously described [13]. A Lake Shore temperature controller was used to monitor the temperature of the sample, incoming transfer lines, and exhaust line.

3. TEMTriPol-1 enhancement profile

To determine the microwave frequency for maximal enhancement with TEMTriPol-1, CPMAS experiments were performed at varying gyrotron frequencies to record the ^{1}H Zeeman enhancement profile of the biradical (Fig. 1a). For these experiments, a polarization time of 3 s was used, even though it is significantly shorter than the optimal polarization time shown in Fig. S3b. At 90 K, 5 mM TEMTriPol-1 yielded a maximum positive enhancement of 76 at a gyrotron frequency of 197.670 GHz with a polarization time of 3 s (Fig. 1b). This profile is similar to that reported previously [29,36].

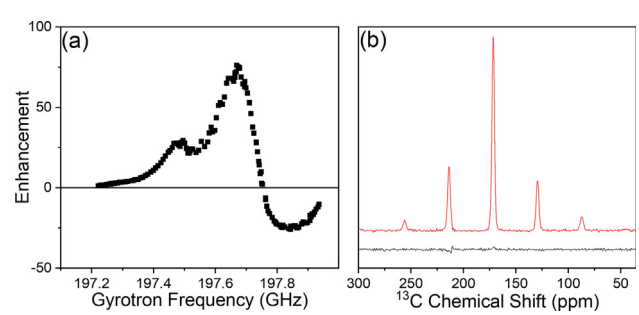

Fig. 1. (a) ^{1}H Zeeman enhancement profile of TEMTriPol-1 at varying gyrotron frequencies. (b) DNP-enhanced CPMAS spectrum at 90 K of 4 M [U-^{13}C,^{15}N] urea with TEMTriPol-1 at 5 mM, $\nu_{rot} = 3200$ Hz. Black represents no DNP, red is with DNP at $\nu_{gyrotron} = 197.670$ GHz. (For interpretation of the references to colour in this figure legend, the reader is referred to the web version of this article.)

4. Sensitivity of trityl at 6 K

To put in perspective the increase in sensitivity at 6 K compared to more conventional temperatures around 90 K, the sensitivity of cross polarization experiments at both temperatures was compared using the solid effect. Fig. 2 shows spectra of 4 M [U-^{13}C,^{15}N] urea with 40 mM trityl. The polarization time for each experiment was chosen to be 1.26 * T_{1DNP} at their respective temperatures (Fig. S1). Since the ^{1}H T_{1DNP} at 90 K was half as long as at 6 K, the number of scans taken at 90 K was doubled to keep the total experimental time the same for both experiments. As can be seen in Fig. 2, the spectrum recorded below 6 K shows much improved signal to noise. The intensity of the ^{13}C Urea resonance is 3.2× larger, indicating a significant improvement to NMR sensitivity available at cryogenic temperatures below 6 K by a factor of 3.2× compared to 90 K.

As discussed below, AMUPol and TEMTriPol-1 affect the sample through depolarization and other deleterious effects, such as paramagnetic relaxation. Note that while TEMTriPol-1 has been shown to not depolarize the sample at temperatures near 100 K, this is not necessarily the case below 6 K, as we will show in the following sections. Trityl is a narrow-line monoradical that does not meet the cross effect condition and thus does not cause depolarization. However, other detrimental effects such as paramagnetic relaxation can remain.

5. Power dependence comparison

CPMAS experiments with varying microwave transmission through the waveguide were performed below 6 K to determine dependence of the maximum ^{1}H signal enhancements for TEMTriPol-1 and AMUPol on the incident microwave power (Fig. 3). Attenuators were inserted into a 9 mm gap in the middle of the corrugated waveguide to modulate the microwave power on the sample. The microwave power on each sample without any attenuators was estimated to be 7 W at a microwave frequency of 197.670 GHz, resulting in an average electron Rabi frequency of 0.45 MHz [22,23]. Lower microwave powers result in lower cross effect DNP enhancement if on-resonance electron spins are not fully saturated. [46,47] The cross effect becomes saturated at about 0.6 W of microwave power using 5 mM TEMTriPol-1 (Fig. 3a). However, in the case of 5 mM AMUPol, increasing microwave power continues to increase NMR signal intensity up to about 5 W of microwave power (Fig. 3b). Therefore, we demonstrate that lower microwave sources are fully suitable for cross effect DNP from biradicals containing a slowly relaxing narrow-line radical, yet gyrotron sources capable of producing > 10 W are advantageous for bi-nitroxide polarizing agents. We observe similar power dependencies at 90 K for both radicals (Fig. S2). The cross effect saturates at higher powers for both radicals at 90 K, but TEMTriPol-1 still saturates at a significantly lower power compared to AMUPol at 90 K.

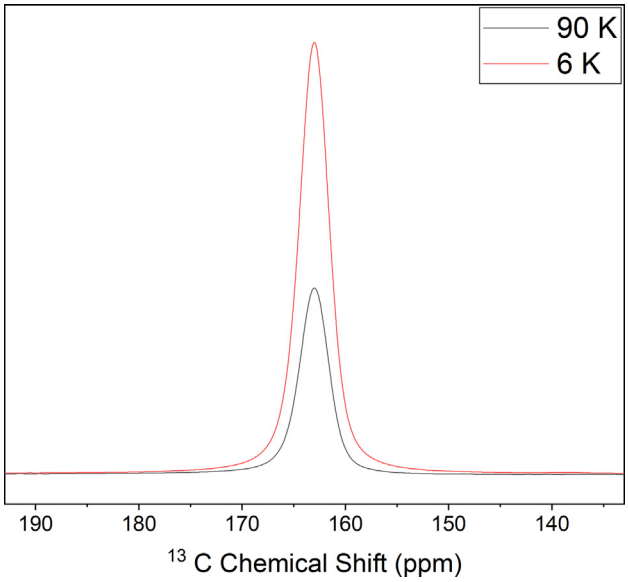

Fig. 2. Comparison of the sensitivity of CPMAS experiments on 4 M [U-^{13}C,^{15}N] urea with 40 mM trityl at 90 K (black) and 6 K (red). The total experimental time to acquire both spectra were the same. (For interpretation of the references to colour in this figure legend, the reader is referred to the web version of this article.)

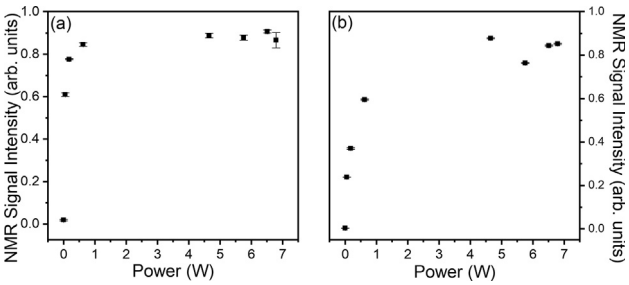

Fig. 3. Area of the [U-^{13}C,^{15}N] urea ^{13}C resonance dependence on relative microwave power below 6 K for (a) TEMTriPol-1 and (b) AMUPol.

6. Signal-to-noise and sensitivity

As described by De Paëpe and colleagues, the signal-to-noise per unit time is the true measure of sensitivity, and depends on many parameters besides DNP enhancement including, but not limited to; temperature, experimental repetition time, noise figures, and signal attenuation due to the presence of radicals [28,29,34,49,50]. Note that, when comparing the sensitivity between two experiments that are not taken over the same amount of time, it is necessary to consider the square root of the polarization time. As such, in our comparison between AMUPol and TEMTriPol-1 in this paper we consider the square root of the polarization time when comparing the sensitivity of both radicals below 6 K. The signal-to-noise per unit time provided by 5 mM AMUPol (Fig. 4a) and 5 mM TEMTriPol-1 (Fig. 4e) were compared from CPMAS experiments below 6 K (Fig. 4). With an incident microwave power of 7 W, 5 mM AMUPol provided an enhancement of 253 at 5.1 K (Fig. 4b). 5 mM TEMTriPol-1 provided a smaller enhancement of 49 at 4.2 K (Fig. 4f). DNP polarization periods of 1.26 * T_{1DNP} were used for each radical.

It is important to note that the signal enhancement with TEMTriPol-1 has been shown here to be greater at 90 K than at 6 K. An explanation for the different behavior of the cross effect for different biradicals is that it is dependent on electronic relaxation times [33]. It was demonstrated by Vega and colleagues that at temperatures below 30 K the cross effect starts to become much less efficient [51]. Neither AMUPol nor TEMTriPol-1 were designed for use at such low temperatures and, as such, their performance at 6 K do not mimic the improvement in sensitivity seen with trityl (Fig. 2).

While the enhancements from AMUPol were significantly larger than TEMTriPol-1, AMUPol reduces the signal obtained from the nuclear spins in the absence of microwaves more substantially than TEMTriPol-1 due to a combination depolarization and other detrimental effects such as paramagnetic relaxation. The extent of the depolarization of AMUPol has been partially attributed to

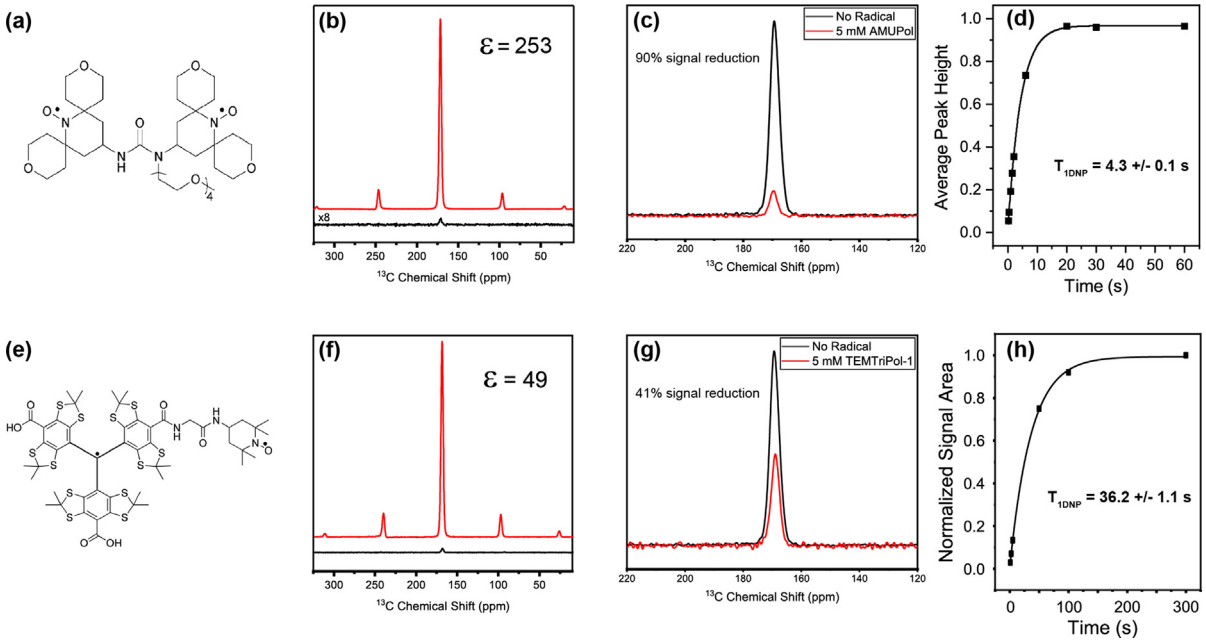

Fig. 4. Structures of AMUPol (a) and TEMTriPol-1 (e) and their corresponding DNP CPMAS spectra of 4 M [U-^{13}C,^{15}N] urea with 5 mM AMUPol (ν_{rot} = 5700 Hz) (b) and 5 mM TEMTriPol-1 (ν_{rot} = 5700 Hz) (f), with the DNP signal in red and the no DNP signal in black. (c) and (g) show the signal reduction of the sample caused by the addition of 5 mM AMUPol and TEMTriPol-1, respectively, with the urea signal with no radical in black and the urea signal with radical in red (ν_{rot} = 5700 Hz). (d) and (h) show the ^{1}H T_{1DNP} polarization buildup times for AMUPol and TEMTriPol-1, respectively. All data was recorded at a microwave power of 7 W below 6 K. (For interpretation of the references to colour in this figure legend, the reader is referred to the web version of this article.)

its longer T_{1e} relaxation times compared to other, non-depolarizing radicals [29,33]. In the case of narrow-line monoradicals such as trityl, these paramagnetic relaxation effects can be mitigated with electron decoupling [24,41]. However, biradicals with extensive inhomogenous broadening will require much higher electron spin Rabi frequencies to implement electron decoupling.

CPMAS experiments were performed in the absence of microwaves below 6 K at 7 T to determine the extent to which the signal was reduced by 5 mM AMUPol compared to 5 mM TEMTriPol-1, which has been shown to not depolarize at 100 K. Urea with 5 mM AMUPol results in only 10% of the intensity compared to urea without radical (Fig. 4c). Markedly, 5 mM TEMTriPol-1 reduces signal to a lesser extent, at 59% of the intensity compared to urea without radical (Fig. 4g). Substituting the radical-present microwave-off signal with its no-radical counterpart, the "adjusted enhancements" were 25 for 5 mM AMUPol and 29 for 5 mM TEMTriPol-1 at an incident microwave power of 7 W [28].

While the adjusted enhancements obtained with 5 mM TEMTriPol-1 and 5 mM AMUPol were more similar in magnitude, the ^{1}H T_1 polarization buildup times (T_{1DNP}) were significantly different. The T_{1DNP} plots for ^{1}H below 6 K are shown in Fig. 4d and h. Urea with 5 mM AMUPol had a short T_{1DNP} time of 4.3 ± 0.1 s (Fig. 4d). In contrast, 5 mM TEMTriPol-1 exhibited a much longer T_{1DNP} time of 36.2 ± 1.1 s (Fig. 4h). Thus, the polarization time required to achieve the maximum enhancement with AMUPol was about 9-times shorter than for TEMTriPol-1. This shorter T_{1DNP} allows AMUPol to provide superior signal-to-noise per unit time. To compare the sensitivity for each radical, the adjusted enhancement was divided by the square root of the corresponding T_{1DNP}. The sensitivity for AMUPol was calculated to be 2.5 times larger than for TEMTriPol-1.

A similar comparison using the signal-to-noise divided by the square root of the polarization time for each radical is shown in Table 1. An extended table is provided in the supplemental information (Table S1). For reference, dividing the signal-to-noise by the square root of the polarization time shows that AMUPol provides 3.1× more signal-to-noise per unit square root time than TEMTriPol-1 at 6 K. At 90 K, AMUPol provides the greatest sensitivity, yielding 1.4× more signal-to-noise per unit square root time than trityl, and 1.7× more than TEMTriPol-1. However, at 6 K trityl yields 1.9× more signal-to-noise per unite square root time than AMUPol, and 6.0× more than TEMTriPol-1 at 7 T. Thus, at 90 K, AMUPol with the cross effect is preferential for obtaining the greatest sensitivity, while at 6 K, trityl is preferable for more sensitive experiments with the solid effect.

Table 1
Sensitivity comparison of AMUPol, TEMTriPol-1, and trityl at 90 K and 6 K. Columns show the signal-to-noise divided by the square root of the polarization buildup time.

Radical (Mechanism)	90 K S/N/sqrt(τ_{pol})	6 K S/N/sqrt(τ_{pol})
AMUPol (CE)	222	261
TEMTriPol-1 (CE)	134	84
Trityl (SE)	156	506

The sensitivity comparison between 90 K and 6 K performed on trityl in section 4 can also be made for the cross effect radicals discussed here. To do so, we compared the signal-to-noise produced by both radicals at each temperature divided by the square root of their respective polarization times (Table 1). Surprisingly, neither AMUPol nor TEMTriPol-1 displayed a significant increase in sensitivity when the sample temperature was reduced to 6 K, with TEMTriPol-1 actually decreasing in sensitivity. AMUPol's signal-to-noise per unit time increased by a factor of only 1.2×, while TEMTriPol-1's sensitivity is only 0.6x compared to 90 K (Table S1). This is in stark contrast to trityl, which increased in sensitivity by 3.2× (Table S1). As mentioned previously, it has already been observed that the cross effect is less efficient at temperatures below 30 K [51]; this decrease in efficiency may be preventing the increase in sensitivity for AMUPol and TEMTriPol-1 that was observed for trityl.

To determine whether the relationship between ^{1}H relaxation times remains the same in the absence of microwaves, we com-

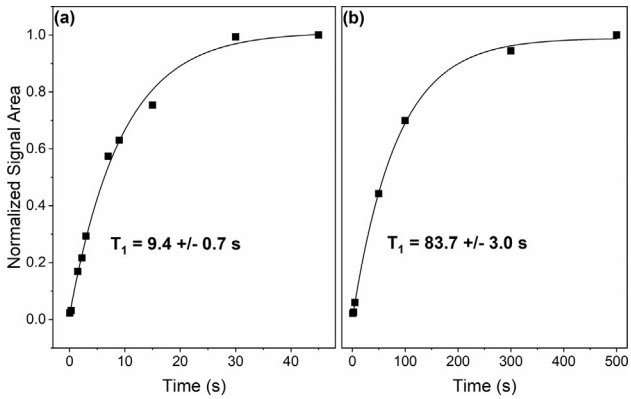

Fig. 5. ^{1}H T_1 of [U-^{13}C,^{15}N] urea with (a) 5 mM AMUPol and (b) 5 mM TEMTriPol-1.

pared the ^{1}H T_1 (without microwaves) of [^{13}C,^{15}N] urea with AMUPol and TEMTriPol-1 (Fig. 5). It was determined that the ^{1}H T_1 with AMUPol was 9.4 ± 0.7 s (Fig. 5a), which is 9 times shorter than the 83.7 ± 3.0 s T_1 we determined for TEMTriPol-1 (Fig. 5b). It is noteworthy that the ^{1}H T_1 and the ^{1}H T_{1DNP} times are not equal for either biradical used, which is not typically observed for biradicals and cross effect DNP. The disparity in T_1 and T_{1DNP} indicates that DNP mechanisms at 6 K and 90 K are not identical [33]. This could be partially due to the difference in electron polarization at 6 K compared to 90 K. The increased polarization at 6 K makes electron-electron pairs with opposite spin orientation to participate in the cross effect less common [56].

7. Conclusions

Here, we definitively demonstrate that solid effect DNP is more sensitive below 6 K than at 90 K by performing CPMAS experiments with trityl. The sensitivity at 6 K was determined to be 3.2× greater than at 90 K. We also show that AMUPol offers significant advantages over TEMTriPol-1 for quickly obtaining improved signal-to-noise below 6 K at 7 T. While AMUPol greatly depolarizes nuclear spins, the adjusted enhancement was still of similar magnitude to that of TEMTriPol-1. Furthermore, the polarization time required to achieve these enhancements drastically favored AMUPol, which required only one ninth the time to provide its maximum enhancement. The shorter T_{1DNP} effectively enables AMUPol to provide 2.5 times more signal-to-noise per unit time. While AMUPol exhibited these clear advantages between the two cross effect radicals, TEMTriPol-1 may still offer its own distinct advantages below 6 K at 7 T. For instance, a chelated gadolinium moiety could be covalently attached to trityl-nitroxide radicals to achieve shorter electron spin relaxation properties [57]. Furthermore, electron decoupling of trityl within TEMTriPol-1 could also mitigate detrimental effects due to the strong hyperfine interactions [24,41]. We have already shown electron decoupling with a trityl radical has the ability to improve the signal intensity while decreasing the linewidth of the signal at temperatures below 6 K [41]. Furthermore, this sensitivity comparison may not scale up to larger magnetic fields (>18 T), where TEMTriPol-1 is known to provide more efficient DNP transfer than at 7 T [29,36].

Trityl yielded the highest sensitivity between all three radicals studied. Using the solid effect, trityl yielded 1.9× and 6.0× more signal-to-noise per unit square root time than the cross effect radicals AMUPol and TEMTriPol-1, respectively, at 6 K and 7 T. Furthermore, we demonstrated that at 6 K the cross effect is saturated at about 5 W of microwave power with 5 mM AMUPol, and at 0.6 W with 5 mM TEMTriPol-1. Since trityl uses the solid effect as its primary DNP mechanism, we do not expect DNP enhancements to diminish with stronger microwave fields, opening the possibility for even greater sensitivity at 6 K with greater microwaves powers. Greater microwave powers will also open the possibility of pulsed DNP for coherent manipulation of electron spins, especially with a narrow-line radical such as trityl. We have successfully performed electron decoupling on trityl below 6 K [41]. We have also demonstrated that we can successfully decouple the hyperfine interactions between the electron spins and nuclear spins in close proximity to the radical [58]. One advantage that TEMTriPol-1 has over trityl, though, is that the solid effect is less effective at fields for which TEMTriPol-1 is optimized (>18 T). This opens the possibility that TEMTriPol-1, or other cross effect radicals designed for operation at high magnetic fields, will yield greater sensitivity at 90 K and/or 6 K.

The overall signal enhancement of 1000× we have demonstrated using MAS DNP < 6 K will benefit structural biology and characterization of materials. For example, determining distance constraints on biochemical structures involves multiple evolution dimensions, leading to currently lengthy experimental times [51–55]. Maximizing the signal-to-noise ratio obtained in an NMR experiment by achieving the largest possible electron Boltzmann polarization, as well as optimizing the efficiency of DNP transfers, allows these experiments to be performed in a fraction of the time required otherwise.

Aside from its *in vitro* applications, AMUPol has also been shown to be effective for enhancing NMR signals in an *in vivo* environment of HEK293-F cells [42]. In-cell DNP experiments will be critical for elucidating the structure-function relationship of many biological systems in their native cellular environment. Maximizing the signal-to-noise of the sparsely-populated NMR spins in these cellular samples through DNP and through cooling the system down to cryogenic temperatures below 6 K will be necessary for such experiments.

There are two distinct routes for improving the MAS DNP-NMR below 6 K. One is to use new radicals for continuous wave DNP transfers that are designed to have optimal relaxation properties. However, we believe continuous wave DNP will evolve into the pulsed regime, as microwave technology is developed and becomes widely available. A second route to ultra-sensitive NMR below 6 K is therefore the application of pulsed microwaves for time-domain transfer mechanisms, followed by pulsed electron decoupling. Therefore, we will develop new instrumentation to implement intense chirped microwave pulses for MAS.

Acknowledgements

This research was supported by the NIH (DP2-GM119131), NSF-IDBR (CAREER DBI-1553577), the Camille Dreyfus Teacher-Scholar Awards Program, the Deutsche Forschungsgemeinschaft (DFG) postdoc fellowship (414196920), and the University of Iceland Research Fund. We thank Brice Albert, Faith Scott, Chukun Gao, and Natalie Golota for assistance building instrumentation.

Appendix A. Supplementary material

Supplementary data to this article can be found online at https://doi.org/10.1016/j.jmr.2019.05.011.

References

[1] T. Polenova, R. Gupta, A. Goldbourt, Magic angle spinning NMR spectroscopy: a versatile technique for structural and dynamic analysis of solid-phase systems, Anal. Chem. 87 (2015) 5458–5469.
[2] A.J. Rossini, C.M. Widdifield, A. Zagdoun, M. Lelli, M. Schwarzwälder, C. Copéret, A. Lesage, L. Emsley, Dynamic nuclear polarization enhanced NMR

spectroscopy for pharmaceutical formulations, J. Am. Chem. Soc. 136 (2014) 2324–2334.
[3] M. Kaplan, S. Narasimhan, C. de Heus, D. Mance, S. van Doorn, K. Houben, D. Popov-Čeleketić, R. Damman, E.A. Katrukha, P. Jain, W.J.C. Geerts, A.J.R. Heck, G. E. Folkers, L.C. Kapitein, S. Lemeer, P.M.P. van Bergen en Henegouwen, M. Baldus, EGFR dynamics change during activation in native membranes as revealed by NMR, Cell 167 (1241–1251) (2016) e11.
[4] S. Hayes, L. Van Wüllen, H. Eckert, W.R. Even, R.W. Crocker, Z. Zhang, Solid-state NMR strategies for the structural investigation of carbon-based anode materials, Chem. Mater. 9 (1997) 901–911.
[5] M.L. Mak-Jurkauskas, V.S. Bajaj, M.K. Hornstein, M. Belenky, R.G. Griffin, J. Herzfeld, Energy transformations early in the bacteriorhodopsin photocycle revealed by DNP-enhanced solid-state NMR, Proc. Natl. Acad. Sci. 105 (2008) 883–888.
[6] A.S.L. Thankamony, J.J. Wittmann, M. Kaushik, B. Corzilius, Dynamic nuclear polarization for sensitivity enhancement in modern solid-state NMR, Prog. Nucl. Magn. Reson. Spectrosc. 120–195 (2017).
[7] M.W. Dale, C.J. Wedge, Optically generated hyperpolarization for sensitivity enhancement in solution-state NMR spectroscopy, Chem. Commun. 52 (2016) 13221–13224.
[8] E.P. Saliba, E.L. Sesti, N. Alaniva, A.B. Barnes, Pulsed electron decoupling and strategies for time domain dynamic nuclear polarization with magic angle spinning, J. Phys. Chem. Lett. 9 (2018) 5539–5547.
[9] T. Maly, G.T. Debelouchina, V.S. Bajaj, K.-N. Hu, C.-G. Joo, M.L. Mak-Jurkauskas, J.R. Sirigiri, P.C.A. van der Wel, J. Herzfeld, R.J. Temkin, R.G. Griffin, Dynamic nuclear polarization at high magnetic fields, J. Chem. Phys. 128 (2008) 052211.
[10] A.B. Barnes, E.A. Nanni, J. Herzfeld, R.G. Griffin, R.J. Temkin, A 250 GHz gyrotron with a 3 GHz tuning bandwidth for dynamic nuclear polarization, J. Magn. Reson. 221 (2012) 147–153.
[11] K.R. Thurber, W.M. Yau, R. Tycko, Low-temperature dynamic nuclear polarization at 9.4 T with a 30 mW microwave source, J. Magn. Reson. 204 (2010) 303–313.
[12] A.N. Smith, M.A. Caporini, G.E. Fanucci, J.R. Long, A method for dynamic nuclear polarization enhancement of membrane proteins, Angew. Chem. Int. Ed. 54 (2015) 1542–1546.
[13] J.M. Franck, A. Pavlova, J.A. Scott, S. Han, Quantitative cw Overhauser effect dynamic nuclear polarization for the analysis of local water dynamics, Prog. Nucl. Magn. Reson. Spectrosc. 74 (2014) 33–56.
[14] A. Leavesley, C.B. Wilson, M. Sherwin, S. Han, Effect of water/glycerol polymorphism on dynamic nuclear polarization, Phys. Chem. Chem. Phys. 20 (2018) 9897–9903.
[15] A. Equbal, Y. Li, A. Leavesley, S. Huang, S. Rajca, A. Rajca, S. Han, Truncated cross effect dynamic nuclear polarization: an overhauser effect doppelgänger, J. Phys. Chem. Lett. 9 (2018) 2175–2180.
[16] L.R. Becerra, G.J. Gerfen, R.J. Temkin, D.J. Singel, R.G. Griffin, Dynamic nuclear polarization with a cyclotron resonance maser at 5 T, Phys. Rev. Lett. 71 (1993) 3561–3564.
[17] D.A. Hall, D.C. Maus, G.J. Gerfen, S.J. Inati, L.R. Becerra, F.W. Dahlquist, R.G. Griffin, Polarization-enhanced NMR spectroscopy of biomolecules in frozen solution, Science 276 (1997) 930–932.
[18] A.W. Overhauser, Polarization of nuclei in metals, Phys. Rev. 92 (1953) 411–415.
[19] Y. Matsuki, T. Idehara, J. Fukazawa, T. Fujiwara, Advanced instrumentation for DNP-enhanced MAS NMR for higher magnetic fields and lower temperatures, J. Magn. Reson. 264 (2016) 107–115.
[20] Y. Matsuki, H. Takahashi, K. Ueda, T. Idehara, I. Ogawa, M. Toda, H. Akutsu, T. Fujiwara, Dynamic nuclear polarization experiments at 14.1 T for solid-state NMR, Phys. Chem. Chem. Phys. 12 (2010) 5799–5803.
[21] A.B. Barnes, E. Markhasin, E. Daviso, V.K. Michaelis, E.A. Nanni, S. Jawla, E.L. Mena, R. DeRocher, A. Thakkar, P. Woskov, J. Herzfeld, R.J. Temkin, R.G. Griffin, Dynamic nuclear polarization at 700 MHz/460 GHz, J. Magn. Reson. 224 (2012) 1–7.
[22] F.J. Scott, E.P. Saliba, B.J. Albert, N. Alaniva, E.L. Sesti, C. Gao, N.C. Golota, E.J. Choi, A.P. Jagtap, J.J. Wittmann, M. Eckardt, W. Harneit, B. Corzilius, S. Th Sigurdsson, A.B. Barnes, Frequency-agile gyrotron for electron decoupling and pulsed dynamic nuclear polarization, J. Magn. Reson. 289 (2018) 45–54.
[23] D.E.M. Hoff, B.J. Albert, E.P. Saliba, F.J. Scott, E.J. Choi, M. Mardini, A.B. Barnes, Frequency swept microwaves for hyperfine decoupling and time domain dynamic nuclear polarization, Solid State Nucl. Magn. Reson. 72 (2015) 79–89.
[24] E.P. Saliba, E.L. Sesti, F.J. Scott, B.J. Albert, E.J. Choi, N. Alaniva, C. Gao, A.B. Barnes, Electron decoupling with dynamic nuclear polarization in rotating solids, J. Am. Chem. Soc. 139 (18) (2017) 6310–6313.
[25] S. Alberti, F. Braunmueller, T.M. Tran, J. Genoud, J.P. Hogge, M.Q. Tran, J.P. Ansermet, Nanosecond pulses in a THz gyrotron oscillator operating in a mode-locked self-consistent q-switch regime, Phys. Rev. Lett. 111 (2013) 205101.
[26] D.S. Wollan, Dynamic nuclear polarization with an inhomogeneously broadened ESR line, Phys. Rev. B 13 (9) (1976) 3671–3685.
[27] K. Hu, H. Yu, T.M. Swager, R.G. Griffin, Dynamic nuclear polarization with biradicals, J. Am. Chem. Soc. 126 (2004) 10844–10845.
[28] F. Mentink-Vigier, S. Paul, D. Lee, A. Feintuch, S. Hediger, S. Vega, G. De Paëpe, Nuclear depolarization and absolute sensitivity in magic-angle spinning cross effect dynamic nuclear polarization, Phys. Chem. Chem. Phys. 17 (2015) 21824–21836.
[29] F. Mentink-Vigier, G. Mathies, Y. Liu, A.-L. Barra, M.A. Caporini, D. Lee, S. Hediger, R.G. Griffin, G. De Paëpe, Efficient cross-effect dynamic nuclear polarization without depolarization in high-resolution MAS NMR, Chem. Sci. 8 (2017) 8150–8163.
[30] K.R. Thurber, R. Tycko, Theory for cross effect dynamic nuclear polarization under magic-angle spinning in solid state nuclear magnetic resonance: the importance of level crossings, J. Chem. Phys. 137 (2012) 084508.
[31] K.R. Thurber, R. Tycko, Perturbation of nuclear spin polarizations in solid state NMR of nitroxide-doped samples by magic-angle spinning without microwaves, J. Chem. Phys. 140 (2014) 184201.
[32] F. Mentink-Vigier, Ü. Akbey, Y. Hovav, S. Vega, H. Oschkinat, A. Feintuch, Fast passage dynamic nuclear polarization on rotating solids, J. Magn. Reson. 224 (2012) 13–21.
[33] A. Lund, A. Equbal, S. Han, Tuning nuclear depolarization under MAS by electron T 1e, Phys. Chem. Chem. Phys. 20 (2018) 23976–23987.
[34] F. Mentink-Vigier, I. Marin-Montesinos, A.P. Jagtap, T. Halbritter, J. Van Tol, S. Hediger, D. Lee, S.T. Sigurdsson, G. De Paëpe, Computationally-assisted design of polarizing agents for dynamic nuclear polarization enhanced NMR: the AsymPol family, J. Am. Chem. Soc. 140 (2018) 11013–11019.
[35] D. Wisser, G. Karthikeyan, A. Lund, G. Casano, H. Karoui, M. Yulikov, G. Menzildjian, A.C. Pinon, A. Purea, F. Engelke, S.R. Chaudhari, D. Kubicki, A.J. Rossini, I.B. Moroz, D. Gajan, C. Copéret, G. Jeschke, M. Lelli, L. Emsley, A. Lesage, O. Ouari, BDPA-nitroxide biradicals tailored for efficient dynamic nuclear polarization enhanced solid-state NMR at magnetic fields up to 21.1 T, J. Am. Chem. Soc. 140 (2018) 13340–13349.
[36] G. Mathies, M.A. Caporini, V.K. Michaelis, Y. Liu, K.-N. Hu, J.L. Zweier, M. Rosay, M. Baldus, R.G. Griffin, Efficient dynamic nuclear polarization at 800 MHz/527 GHz with trityl-nitroxide biradicals, Angew. Chem. Int. Ed. 54 (2015) 11770–11774.
[37] E.L. Sesti, N. Alaniva, P.W. Rand, E.J. Choi, B.J. Albert, E.P. Saliba, F.J. Scott, A.B. Barnes, Magic angle spinning NMR below 6 K with a computational fluid dynamics analysis of fluid flow and temperature gradients, J. Magn. Reson. 286 (2017) 1–9.
[38] B.J. Albert, S.H. Pahng, N. Alaniva, E.L. Sesti, P.W. Rand, E.P. Saliba, F.J. Scott, E.J. Choi, A.B. Barnes, Instrumentation for cryogenic magic angle spinning dynamic nuclear polarization using 90 L of liquid nitrogen per day, J. Magn. Reson. 283 (2017) 71–78.
[39] D. Lee, E. Bouleau, P. Saint-Bonnet, S. Hediger, G. De Paëpe, Ultra-low temperature MAS-DNP, J. Magn. Reson. 264 (2016) 116–124.
[40] K.R. Thurber, A. Potapov, W.M. Yau, R. Tycko, Solid state nuclear magnetic resonance with magic-angle spinning and dynamic nuclear polarization below 25 K, J. Magn. Reson. 226C (2013) 100–106.
[41] E.L. Sesti, E.P. Saliba, N. Alaniva, A.B. Barnes, Electron decoupling with cross polarization and dynamic nuclear polarization below 6 K, J. Magn. Reson. 295 (2018) 1–5.
[42] B.J. Albert, C. Gao, E.L. Sesti, E.P. Saliba, N. Alaniva, F.J. Scott, S.T. Sigurdsson, A. B. Barnes, Dynamic nuclear polarization nuclear magnetic resonance in human cells using fluorescent polarizing agents, Biochemistry 57 (2018) 4741–4746.
[43] E. Bouleau, P. Saint-bonnet, F. Mentink-vigier, H. Takahashi, J. Jacquot, M. Bardet, F. Aussenac, A. Purea, F. Engelke, S. Hediger, D. Lee, G. De Paëpe, Pushing NMR sensitivity limits using dynamic nuclear polarization with closed-loop cryogenic helium sample spinning, Chem. Sci. 6 (2015) 6806–6812.
[44] F.J. Scott, N. Alaniva, N.C. Golota, E.L. Sesti, E.P. Saliba, L.E. Price, B.J. Albert, P. Chen, R.D. O'Connor, A.B. Barnes, A versatile custom cryostat for dynamic nuclear polarization supports multiple cryogenic magic angle spinning transmission line probes, J. Magn. Reson. 297 (2018) 23–32.
[45] D. Massiot, F. Fayon, M. Capron, I. King, S. Le Calvé, B. Alonso, J.O. Durand, B. Bujoli, Z. Gan, G. Hoatson, Modelling one- and two-dimensional solid-state NMR spectra, Magn. Reson. Chem. 40 (2002) 70–76.
[46] T.A. Siaw, A. Leavesley, A. Lund, I. Kaminker, S. Han, A versatile and modular quasi optics-based 200 GHz dual dynamic nuclear polarization and electron paramagnetic resonance instrument, J. Magn. Reson. 264 (2016) 131–153.
[47] H. Takahashi, C. Fernández-de-alba, D. Lee, V. Maurel, S. Gambarelli, M. Bardet, S. Hediger, A. Barra, G. De Paëpe, Optimization of an absolute sensitivity in a glassy matrix during DNP-enhanced multidimensional solid-state NMR experiments, J. Magn. Reson. 239 (2014) 91–99.
[48] A.E. Bennett, C.M. Rienstra, M. Auger, K.V. Lakshmi, R.G. Griffin, Heteronuclear decoupling in rotating solids, J. Chem. Phys. 103 (16) (1995) 6951–6958.
[49] H. Takahashi, D. Lee, L. Dubois, M. Bardet, S. Hediger, G. De Paëpe, Rapid natural-abundance 2D 13 C – 13 C correlation spectroscopy using dynamic nuclear polarization enhanced solid-state NMR and matrix- free sample preparation, Angew. Chem. Int. Ed. (2012) 11766–11769.
[50] A.E. Bennett, C.M. Rienstra, J.M. Griffiths, W. Zhen, P.T. Lansbury, R.G. Griffin, Homonuclear radio frequency-driven recoupling in rotating solids, J. Chem. Phys. 108 (1998) 9463–9479.
[51] D. Shimon, Y. Hovav, A. Feintuch, D. Goldfarb, S. Vega, Dynamic nuclear polarization in the solid state: a transition between the cross effect and the solid effect, Phys. Chem. Chem. Phys. 14 (2012) 5729–5743.
[52] N.M. Szeverenyi, M.J. Sullivan, G.E. Maciel, Observation of spin exchange by two-dimensional fourier transfrom 13C cross polarization-magic-angle spinning, J. Magn. Reson. 47 (1982) 462–475.
[53] S. Grzesiek, A. Bax, Improved 3D triple-resonance NMR techniques applied to a 31 kDa protein, J. Magn. Reson. 96 (1992) 432–440.
[54] J.D. Gross, P.R. Costa, J.P. Dubacq, D.E. Warschawski, P.N. Lirsac, P.F. Devaux, R. G. Griffin, J. Magn. Reson. Ser. B 106 (1995) 187–190.

[55] A.B. Barnes, B. Corzilius, M.L. Mak-Jurkauskas, L.B. Andreas, V.S. Bajaj, Y. Matsuki, M.L. Belenky, J. Lugtenburg, J.R. Sirigiri, R.J. Temkin, J. Herzfeld, R.G. Griffin, Resolution and polarization distribution in cryogenic DNP/MAS experiments, Phys. Chem. Chem. Phys. 12 (2010) 5681–5687.
[56] H.Y. Chen, R. Tycko, Temperature-dependent nuclear spin relaxation due to paramagnetic dopants below 30 K: relevance to DNP-enhanced magnetic resonance imagin, J. Phys. Chem. B. 122 (2018) 11731–11742.
[57] A. Lund, A. Equbal, S. Han, Tuning nuclear depolarization under MAS by electron T_{1e}, Phys. Chem. Chem. Phys. 20 (2018) 23976–23987.
[58] N. Alaniva, E.P. Saliba, E.L. Sesti, P.T. Judge, A.B. Barnes, Electron decoupling with chirped microwave pulses for rapid signal acquisition and electron saturation recovery, Angew. Chem. Int. Ed. (2019), https://doi.org/10.1002/anie.201900139.